1994 ANS Reactor Physics Top. Mtg., Knoxville
CV ref P43
April 11-15

ESTIMATES OF RELATIVE CHANGE IN AXIAL LEAKAGE DUE TO VOIDING IN A CANDU REACTOR

Jeremy J. Whitlock [a]
Michael S. Milgram [b,a]
William J. Garland [a]

[a] McMaster University, Department of Engineering Physics, Hamilton, Ontario, Canada, L8S 4L7, (905) 525-9140

[b] AECL Research, Reactor Physics Branch, Chalk River, Ontario, Canada, KOJ 1JO, (613) 584-8811

KEYWORDS: Leakage, Monte Carlo, CANDU

ABSTRACT

The Monte-Carlo method and a deterministic method are used to estimate the relative perturbation in axial leakage from a lattice cell upon complete and instantaneous coolant voiding. With a Monte-Carlo code the ratio of net current tallies at the axial boundary of the fuel channel is calculated and compared with estimates from a two-dimensional deterministic lattice code, using estimated axial bucklings and two different methods for calculating the diffusion coefficient. Results are grouped into four energy bins.

INTRODUCTION

It is important to be able to accurately model each of the component mechanisms that contribute to positive reactivity feedback induced by coolant voiding in an operating CANDU[c] reactor. These mechanisms comprise a complicated mixture of spectral and spatial effects[1,2], thought to include a change in neutron leakage from the core. Leakage is expected to increase upon voiding since spectrum hardening and increased streaming both lead to larger cell diffusion coefficients. Generally, infinite-lattice cell codes (like WIMS-AECL[3]), which provide these coefficients, are not designed to implicitly account for core boundary effects and require an explicit adjustment in the form of user-supplied buckling values. In this paper we investigate the accuracy of this methodology by comparing estimates of relative change in axial leakage upon 100% instantaneous coolant voiding in CANDU, using WIMS-AECL and the Monte-Carlo code MCNP-4[4]. Since MCNP-4 is a much more fundamental code this can be considered a benchmark study of WIMS-AECL, within the statistical accuracy of our MCNP-4 results. The routine application of Monte-Carlo codes to extended criticality problems such as that described here, made possible by advances in computer hardware, is a powerful addition to the suite of analysis tools available to the reactor physicist. Previous studies of CANDU void reactivity in both infinite and finite geometries using MCNP-4 have been reported elsewhere[5,6].

---

[c] CANDU: CANada Deuterium Uranium. Registered Trademark.

DESCRIPTION OF WIMS-AECL AND MCNP-4

WIMS-AECL uses collision-probabilities to solve the multi-group neutron transport equation in a two-dimensional infinite lattice (the PIJ transport option was used here). It has been developed by AECL from a version of WIMS provided by the UKAEA in 1971. Diffusion coefficients can be calculated using either the Benoist method[7,8] or a simple transport calculation[9], and both methods have been used in this paper. The ENDF/B-V WIMS cross-section library was used in its full 89-group format. MCNP-4 is a stochastic (Monte-Carlo) three-dimensional particle tracking code, used in analog neutron transport mode with a continuous-energy cross-section library also derived from ENDF/B-V. Both codes were run on a workstation.

DESCRIPTION OF MODEL

The lattice cell for WIMS-AECL and MCNP-4 was a cylindrical 37-element CANDU fuel bundle surrounded by fuel channel material and moderator with a square reflective boundary of side 28.55 cm (see also References 5 and 6), shown in Figure 1(a). D_2O coolant and moderator temperature (600 K and 300 K, respectively) corresponded to MCNP-4 library values. Fuel temperature (300 K) also corresponded to the nominal MCNP-4 library value, to avoid concerns[5] about temperature modelling.

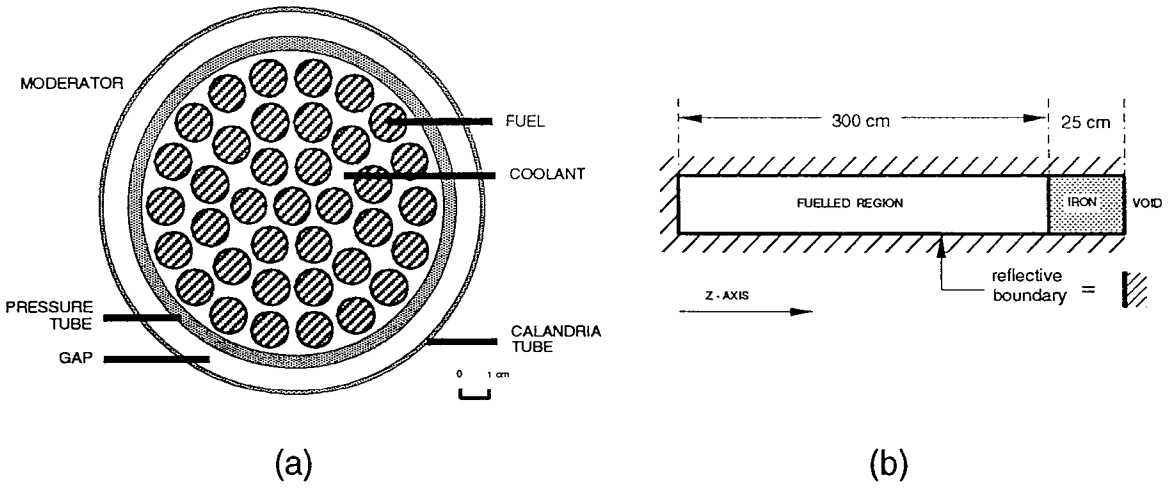

Figure 1. (a) 37-Element CANDU Lattice Cell; (b) Axial Model Used in MCNP-4

Axial CANDU geometry was modelled in MCNP-4 by six adjacent 50.0 cm fuel bundles in a 300.0 cm half-channel, terminated by a 25.0 cm iron slab at one end and a reflection symmetry plane at the other, as shown in Figure 1(b). A void region of zero importance terminated this geometry axially. Partial currents were tallied at the plane interface between the fuelled and termination regions. Additional calculations used unrealistic half-channel lengths of 125.0 cm and 60.0 cm in order to improve tally statistics at this interface[10]. In WIMS-AECL these varying channel lengths were reflected in energy-independent axial bucklings derived from MCNP-4 using the method of Reference 10. These bucklings are listed in Table 1, along with diffusion theory bare-core values[9] for comparison. Since the estimation of collision probabilities in any 2-D lattice code such as WIMS-AECL includes an axial integration to infinity, the adequacy of such a code's radial flux calculation should decrease with shorter fuel channels. For example, the cell diffusion length in CANDU is on the order of 20 cm and therefore one would

suspect the accuracy of a flux solution for the 60 cm half-channel case; however, the relative perturbation in axial leakage upon voiding should be unaffected.

Table 1. Axial Bucklings Derived for WIMS-AECL (accuracy ± 0.2%)

Total Channel Length	Cooled Case (cm-2)	Voided Case (cm-2)	Theoretical Value (cm-2)
600 cm	2.59×10^{-5}	2.60×10^{-5}	2.74×10^{-5}
250 cm	1.39×10^{-4}	1.38×10^{-4}	1.58×10^{-4}
120 cm	5.59×10^{-4}	5.52×10^{-4}	6.85×10^{-4}

DESCRIPTION OF METHOD

The subject of interest in this study is the accuracy of the relative change in axial leakage upon 100% instantaneous voiding,

$$R \equiv \frac{\left(L_z^{voided\,100\%} - L_Z^{cooled}\right)}{L_z^{cooled}} \quad , \tag{1}$$

where L_Z is net surface-integrated leakage, defined by Equation (2):

$$L_Z \equiv \int_S \left(J_Z^+ - J_Z^-\right)\cdot ds = L_Z^+ - L_Z^- \quad . \tag{2}$$

Here S denotes the axial surface area. The surface-integrated partial currents, L^+_Z and L^-_Z, can be calculated directly using the direction cosine current tally option in MCNP-4, which normalizes the tallies to one starting neutron. The statistical uncertainty in L_Z is reduced by $2cov(L^+_Z, L^-_Z)$, the error correlation term associated with the partial currents, which can be extracted from MCNP-4 indirectly[10]. The statistical errors in the tallies for the two cases (cooled and voided) are assumed to be uncorrelated.

In WIMS-AECL leakage is treated by a user-supplied geometric buckling. Two-dimensional collision probabilities integrated to infinity in the axial direction account for an average over the third dimension, so that axial leakage can be estimated using classical diffusion theory (assuming D_Z is independent of z),

$$L_Z \approx -\int_V D_Z \nabla^2 \phi \, dV = V D_Z B_Z^2 \overline{\phi} \quad . \tag{3}$$

The cell-averaged neutron flux, $\overline{\phi}$, was normalized to a unit source in accordance with the normalization

in MCNP-4. The axial diffusion coefficient, D_Z, was calculated with and without the Benoist method selected (the code default is a simple transport calculation). Note that the bucklings listed in Table 1 are virtually independent of voiding, and therefore the ratio in Equation (1) is affected mainly by the change in cell diffusion coefficient and flux.

RESULTS AND DISCUSSION

After 24 million neutron histories (24 Mh) the MCNP-4 values of k_{eff} and k_∞ (using the correlated value from three different estimates[4]) converged to the values in Table 2, compared there with the corresponding WIMS-AECL results. Despite an overall discrepancy of 5 mk (0.5%) in criticality between the two codes (thought to be related to differences in temperature treatment), there is excellent agreement in the predictions of void reactivity (Δk_{eff} or Δk_∞), including the WIMS-AECL case without the Benoist option. The presence of a constant 5 mk discrepancy between the two codes in both the k_{eff} and k_∞ calculations demonstrates that the overestimation by the lattice code is not due to the finite axial geometry.

Table 2. Comparison of Criticality and Void Reactivity Between MCNP-4 and WIMS-AECL for 600 cm Fuel Channel

	WIMS-AECL			MCNP-4 (error = σ)	
	k_{eff} with Benoist	k_{eff} without Benoist	k_∞	k_{eff}	k_∞
cooled	1.1223	1.1227	1.1328	1.1175 ± .0001	1.1284 ± .0001
voided	1.1441	1.1449	1.1555	1.1395 ± .0001	1.1503 ± .0001
void reactivity (Δk_{eff} or Δk_∞)	21.8 mk	22.2 mk	22.7 mk	22.0 ± .1 mk	21.9 ± .1 mk

The relative changes in axial leakage upon voiding, calculated with MCNP-4 (24 Mh) and WIMS-AECL using Equations (2) and (3), respectively, are given in Table 3 for four energy bins. Although similar energy bins were used for both codes, the respective cross-section libraries do have different low-energy and high-energy cut-off points: 2×10^{-3} eV to 10 MeV for WIMS-AECL, and 10^{-5} eV to 20 MeV for MCNP-4. This is not significant since about 0.1% of the net current has energy below the WIMS-AECL low-energy cut-off point (estimated from an auxiliary MCNP-4 run) and about 0.1% of the fission spectrum[9] is above the WIMS-AECL high-energy cut-off point.

Both codes calculate a slight decrease in thermal group axial leakage upon voiding, along with increases of approximately 10% and 30% in the resonance and fast groups, respectively. With Benoist diffusion coefficients the increase in total axial leakage (bottom row) calculated by WIMS-AECL is twice the amount calculated by MCNP-4. The results for the subdivided energy groups suggest that a modelling problem occurs in the resonance range, while the results for the thermal and fast groups are satisfactory. When the simple transport calculation for the diffusion coefficient is used the results are almost a

Table 3. Relative Change in Axial Leakage Upon Coolant Voiding for 600 cm Fuel Channel

Energy Group	WIMS-AECL		MCNP-4
	with Benoist	without Benoist	(error = σ)
thermal (0 - 0.625 eV)	– 1.2 %	– 5.1 %	– (1.2 ± 0.3) %
resonance (0.625 eV - 0.821 MeV)	+ 12.2 %	+ 7.5 %	+ (8.0 ± 1.4) %
fast (0.821 MeV - 10 MeV)	+ 34.7 %	+ 30.3 %	+ (33.1 ± 1.8) %
total (0 - 10 MeV)	+ 6.0 %	+ 1.8 %	+ (2.6 ± 0.3) %

complement of those using the Benoist method: the resonance group result agrees with MCNP-4 while the thermal and fast groups do not (although the fast group result is still within the 95% (±2σ) confidence interval of MCNP-4), and the total change in axial leakage is just inside the 99.7% (±3σ) confidence interval.

The results using a 250 cm and 120 cm channel are listed in Table 4 and Table 5, respectively. While absolute leakage would be higher in these geometries, the relative perturbation upon voiding should remain fairly constant since it is primarily a function of material properties. This is reflected in the MCNP-4 results for all three channel lengths (Table 3 to Table 5), with the exception of an anomaly in the thermal group for the 250 cm channel (Table 4). Aside from this anomaly the results for all energy bins do increase slightly with decreasing channel length, but not by more than 3σ from the 600 cm channel case.

Note that the 120 cm channel results (Table 5) show very good agreement between WIMS-AECL (with Benoist diffusion coefficients) and MCNP-4 in all four energy bins. The MCNP-4 statistics are, as expected, best for this case, despite the fact that 12 Mh were run instead of 24 Mh as in the other two cases. Based upon these results we can look back at the 600 cm channel results in Table 3 and suspect that the MCNP-4 calculation, especially for total leakage, had not yet converged satisfactorily. This demonstrates the need for extraordinary long runtimes when such small perturbations are involved.

In the interest of completeness the values of k_{eff} and Δk_{eff} for the two short channel cases are included in Table 6. The trend of overestimation in absolute criticality by WIMS-AECL continues, and in these cases the disagreement in void reactivity is pronounced. This is due to an increase in the relative importance of leakage over absorption as a loss mechanism.

Some light can be shed upon the relative changes in axial leakage in Table 3, by splitting the relative leakage changes into the constituents which change upon voiding — the cell diffusion coefficient, average flux and buckling in Equation (3). These partial contributions, R_D, R_ϕ and R_B (where $R_a \equiv (\partial a/a)$ + second-order Taylor series term), appear in Table 7 and Table 8 for the longest and shortest channels,

Table 4. Relative Change in Axial Leakage Upon Coolant Voiding for 250 cm Fuel Channel

Energy Group	WIMS-AECL		MCNP-4
	with Benoist	without Benoist	(error = σ)
thermal (0 - 0.625 eV)	– 2.7 %	– 6.5 %	– (0.1 ± 0.2) %
resonance (0.625 eV - 0.821 MeV)	+ 10.5 %	+ 5.8 %	+ (8.9 ± 0.7) %
fast (0.821 MeV - 10 MeV)	+ 32.7 %	+ 28.2 %	+ (31.3 ± 0.8) %
total (0 - 10 MeV)	+ 4.5 %	+ 0.4 %	+ (3.7 ± 0.2) %

Table 5. Relative Change in Axial Leakage Upon Coolant Voiding for 120 cm Fuel Channel

Energy Group	WIMS-AECL		MCNP-4
	with Benoist	without Benoist	(error = σ)
thermal (0 - 0.625 eV)	– 2.9 %	– 6.6 %	– (2.1 ± 0.2) %
resonance (0.625 eV - 0.821 MeV)	+ 10.4 %	+ 5.2 %	+ (10.4 ± 0.2) %
fast (0.821 MeV - 10 MeV)	+ 32.8 %	+ 27.6 %	+ (28.3 ± 0.5) %
total (0 - 10 MeV)	+ 4.9 %	+ 0.6 %	+ (3.5 ± 0.1) %

respectively. For WIMS-AECL it is a trivial matter to generate the data in these tables; for MCNP-4 we must average quantities over the axial direction and, in the case of diffusion coefficient[9] and buckling[10], make some estimations based on diffusion theory:

$$\phi(z) \approx 2\left[J_Z^+(z) + J_Z^-(z)\right] \quad ; \quad \overline{\phi} = \frac{\int_Z \phi(z)}{\int_Z dz} \quad ; \quad D_Z \approx \frac{L_Z}{V B_Z^2 \overline{\phi}} \quad . \tag{4}$$

Accuracy estimates for MCNP-4 average flux and diffusion coefficient have been based on the MCNP-4

error for the partial currents, and on the accuracy estimate for B_z^2 (± 0.2%).

Table 6. Comparison of k_{eff} Between MCNP-4 and WIMS-AECL for 250 cm and 120 cm Fuel Channel

		WIMS-AECL		MCNP-4
		with Benoist	without Benoist	(error = σ)
250 cm	cooled	1.0778	1.0796	1.0730 ± .0001
	voided	1.0966	1.1006	1.0927 ± .0001
	void reactivity (Δk_{eff})	18.8 mk	21.0 mk	19.7 ± .1 mk
120 cm	cooled	0.9336	0.9392	0.9295 ± .0002
	voided	0.9428	0.9557	0.9436 ± .0002
	void reactivity (Δk_{eff})	9.2 mk	16.5 mk	14.1 ± .3 mk

It can be seen that all energy groups experience an increase in the cell diffusion parameter upon coolant voiding, and that the drop in thermal leakage is due to a drop in thermal cell flux. The comparison between the two codes indicates that WIMS-AECL (with Benoist option) overestimates the increase in diffusion coefficient for all energy groups, but the effect is not significant for the low-leakage cases corresponding to an operating CANDU reactor. The perturbations in cell flux predicted by WIMS-AECL have a negative bias in comparison with the corresponding MCNP-4 values, indicating that its calculation of voided flux could be too low. These trends are true for both channel lengths, although the overall leakage perturbations for the shortest channel case are similar for the two codes, as noted earlier. An earlier experimental work[11] on D_2O coolant voiding in a natural UO_2 lattice predicts a value of 9% for total $\delta D_z/D$ based upon the ratio of void volume to cell volume (but different geometry).

CONCLUSION

In general we find reasonable agreement between MCNP-4 and WIMS-AECL in terms of estimating axial leakage perturbation upon lattice cell voiding, particularly for cases of direct interest to operating CANDU reactors. An overestimate of the WIMS-AECL change in diffusion coefficient and a negative bias in the flux change, both in comparison with MCNP-4, appear to cancel. The importance of ensuring adequate convergence of the Monte-Carlo process is demonstrated, as is the enormous dedication of CPU time that is required. For these reasons it is clear that we describe a benchmark procedure here and not a routine analysis method. The inadequacy of two-dimensional lattice codes in certain finite geometries is noted.

Table 7. Contribution of Leakage Components to Relative Change in Axial Leakage for 600 cm Fuel Channel

	WIMS-AECL (With Benoist)				WIMS-AECL (Without Benoist)			
Energy Group	R_D	R_ϕ	R_B (derived from MCNP-4)	Total ($R=\sum R_i$)	R_D	R_ϕ	R_B (derived from MCNP-4)	Total ($R=\sum R_i$)
thermal (0 - .625 eV)	+ 6.0 %	– 7.6 %	+ 0.4 %	– 1.2 %	+ 1.9 %	– 7.4 %	+ 0.4 %	– 5.1 %
resonance (.625 eV - .821 MeV)	+ 9.5 %	+ 2.3 %	+ 0.4 %	+ 12.2 %	+ 4.8 %	+ 2.3 %	+ 0.4 %	+ 7.5 %
fast (.821 - 10 MeV)	+ 18.4 %	+ 15.9 %	+ 0.4 %	+ 34.7 %	+ 14.2 %	+ 15.7 %	+ 0.4 %	+ 30.3 %
total (0 - 10 MeV)	+ 9.6 %	– 4.0 %	+ 0.4 %	+ 6.0 %	+ 5.4 %	– 4.0 %	+ 0.4 %	+ 1.8 %

	MCNP-4			
Energy Group	R_D	R_ϕ	R_B	Total ($R=\sum R_i$)
thermal (0 - .625 eV)	+ (3.7 ± 0.3) %	– (5.3 ± 0.01) %	+ (0.4 ± 0.3) %	– (1.2 ± 0.4) %
resonance (.625 eV - .821 MeV)	+ (3.1 ± 1.4) %	+ (4.5 ± 0.02) %	+ (0.4 ± 0.3) %	+ (8.0 ± 1.4) %
fast (.821 - 10 MeV)	+ (12.7 ± 1.5) %	+ (19.5 ± 0.03) %	+ (0.4 ± 0.3) %	+ (33.1 ± 1.6) %
total (0 - 10 MeV)	+ (3.9 ± 0.3) %	– (1.8 ± 0.01) %	+ (0.4 ± 0.3) %	+ (2.6 ± 0.4) %

Table 8. Contribution of Leakage Components to Relative Change in Axial Leakage for 120 cm Fuel Channel

	WIMS-AECL (With Benoist)				WIMS-AECL (Without Benoist)			
Energy Group	R_D	R_ϕ	R_B (derived from MCNP-4)	Total ($R=\sum R_j$)	R_D	R_ϕ	R_B (derived from MCNP-4)	Total ($R=\sum R_j$)
thermal (0 - .625 eV)	+ 5.9 %	– 7.5 %	– 1.3 %	– 2.9 %	+ 2.0 %	– 7.3 %	– 1.3 %	– 6.6 %
resonance (.625 eV - .821 MeV)	+ 9.4 %	+ 2.3 %	– 1.3 %	+ 10.4 %	+ 4.8 %	+ 1.7 %	– 1.3 %	+ 5.2 %
fast (.821 - 10 MeV)	+ 18.1 %	+ 16.0 %	– 1.3 %	+ 32.8 %	+ 13.9 %	+ 15.0 %	– 1.3 %	+ 27.6 %
total (0 - 10 MeV)	+ 9.8 %	– 3.6 %	– 1.3 %	+ 4.9 %	+ 5.7 %	– 3.8 %	– 1.3 %	+ 0.6 %

	MCNP-4			
Energy Group	R_D	R_ϕ	R_B	Total ($R=\sum R_j$)
thermal (0 - .625 eV)	+ (4.8 ± 0.2) %	– (5.5 ± 0.01) %	– (1.3 ± 0.3) %	– (2.1 ± 0.3) %
resonance (.625 eV - .821 MeV)	+ (7.9 ± 0.2) %	+ (3.8 ± 0.02) %	– (1.3 ± 0.3) %	+ (10.4 ± 0.3) %
fast (.821 - 10 MeV)	+ (10.4 ± 0.5) %	+ (18.9 ± 0.03) %	– (1.3 ± 0.3) %	+ (28.3 ± 0.5) %
total (0 - 10 MeV)	+ (6.6 ± 0.1) %	– (1.7 ± 0.01) %	– (1.3 ± 0.3) %	+ (3.5 ± 0.3) %

ACKNOWLEDGEMENTS

This work was partially funded by grants from the Natural Sciences and Engineering Council of Canada, and the CANDU Owners Group.

REFERENCES

1. J. GRIFFITHS, "Lattice Characteristics that Influence the Change in Reactivity with Coolant Voiding in CANDU Lattices," *Proceedings of the 13th Annual Simulation Symposium of the CNS*, AECL Research — Chalk River Laboratories (1987).

2. A. R. DASTUR and D. B. BUSS, "The Influence of Lattice Structure and Composition on the Coolant Void Reactivity in CANDU," *Proceedings of the 11th Annual Conference of the CNS*, Toronto (1990).

3. J. V. DONNELLY, *WIMS-CRNL — A User's Manual For The Chalk River Version of WIMS*, AECL-8955, AECL Research (1986).

4. RSIC Computer Code Collection, *MCNP-4 — Monte Carlo Neutron and Photon Transport Code System*, CCC-200A/B, Oak Ridge National Laboratory (1991).

5. M. S. MILGRAM, "Void Reactivity Predictions for an Infinite Lattice of 37-Element CANDU Fuel", *Proceedings of the Fourth International Conference on Simulation Methods in Nuclear Engineering*, Montreal (1993).

6. M. S. MILGRAM, *Trans. Am. Nucl. Soc.*, **69**, 471 (1993).

7. P. BENOIST, *Nucl. Sci. Eng.*, **77**, 1 (1981).

8. Y. RONEN, *Handbook of Nuclear Reactor Calculations*, Vol. II, CRC Press Inc., Boca Raton, Florida (1986).

9. J. J. DUDERSTADT and L. J. HAMILTON, *Nuclear Reactor Analysis*, John Wiley and Sons, Inc., New York (1976).

10. M. S. MILGRAM, "Determination of Axial Diffusion Coefficients by the Monte-Carlo Method", presented at the *INS/ENS International Conference on Reactor Physics and Reactor Computations*, Tel Aviv (1994).

11. H. R. FIKE and W. E. GRAVES, *Trans. Am. Nucl. Soc.*, **6**, 245 (1963).